Electronic Supplementary Material (ESI) for Nanoscale Advances.

Supplementary Information for

Size-dependent shape distributions of platinum nanoparticles

Ruikang Ding*[1], Ingrid Padilla Espinosa*[2], Dennis Loevlie[3], Soodabeh Azadehranjbar[1], Andrew J. Baker[1], Giannis Mpourmpakis[3], Ashlie Martini[2], Tevis D. B. Jacobs[1]

1) Department of Mechanical Engineering and Materials Science, University of Pittsburgh, Pittsburgh, PA 15261, USA
2) Department of Mechanical Engineering, University of California, Merced, Merced, CA 95340, USA
3) Department of Chemical and Petroleum Engineering, University of Pittsburgh, Pittsburgh, PA 15261, USA

Email: tjacobs@pitt.edu

S1. Literature Review for the Size and Shape of Nanoparticles

A wide variety of simulations and experiments have examined the observed shapes. A sampling of these prior studies reporting sizes and shapes of FCC metal nanoparticles are summarized in Table S1. The stable shapes that were observed range from cubes to octahedra to truncated octahedra to icosahedra, dodecahedra, spheres, and other shapes. These prior studies are extremely useful in predicting different possible shapes, but most do not take into account thermal effects or size-dependence. The purpose of the present paper is not to predict what specific shape the particles will take, which depends sensitively on synthesis conditions, but rather to explore the effect of thermal energy on distributions of shapes.

Table 1: A summary of some of the predicted or measured shapes from prior experimental and simulation investigations.

Size [nm]	Material	Predicted Shape	Other Stable Shapes	Method	References
4.8 - 5.1	Pt	Truncated octahedra	Cubic, octahedra, spheres	MD	(Wen et al., 2009)[1]
3-18	Pt	Octahedra	Dodecahedra, tetrahexahedra, cube, trapezohedra, octahedra, trisohectahedra	MD	(Huang et al., 2011)[2]
1.6 - 6.0	Au	Truncated octahedra		MD	(Shim et al., 2002)[3]
10- 10000 atoms	Ag, Cu, Au, Pd, Pt	Icosahedra	Decahedra for medium sizes, truncated octahedra for large sizes	MD	(Baletto et al., 2002)[4]
3-100	Au	Icosahedra and decahedra	Truncated octahedron for particles > 3 nm	First principles calculation, experimental	(Barnard et al., 2005)[5]
2.2 – 6.3	Au	Icosahedra	Decahedra, truncated octahedra for larger sizes	MD, experimental	(Fleury et al., 2015)[6]
2-25	Cu, Ag, Au, Pd	Icosahedra	Dodecahedra, or truncated octahedra are predominant depending on size and material	MD, Monte Carlo method	(Magnus Rahm & Erhart, 2017)[7]
3-18	Au	Icosahedra	Decahedra with non-spherical truncated bi-pyramid shape for large size	Experimental	(Koga & Sugawara, 2003)[8]

S2. Polyhedral Models & Geometric Measurements

We selected 14 polyhedron models most likely to fit the nanoparticle shapes observed experimentally. Fig. S1 shows all these models. The polyhedra were constructed by only considering <111>, <110>, and <100> facets, which are the most stable facets in an FCC crystal.[9] All facets belonging to the same family had identical surface energy. According to Wulff-construction theory, the distance from the geometric center of the particle to the facet is proportional to the surface energy of the facet.[10] In this way, 11 polyhedra were predicted, as shown in the first four rows of Fig S1. The last row shows polyhedra that do not follow the conventional Wulff construction. The tetrahedron and truncated tetrahedron are considered since they are commonly observed due to the high stability of <111> facets. The icosahedron is composed of 20 tetrahedron units with a twinned structure to accommodate the five-fold symmetry.[11]

The 2D projected shapes of these polyhedra, as viewed along the <100>, <110> and <111> directions, are shown in Fig. S1. Only shapes viewed from the <110> direction can be uniquely determined, since other viewing directions contain cases where a 2D-projected shape may correspond to several possible 3D polyhedra. For instance, the <100> projected shapes of the truncated octahedron and the truncated cuboctahedron are both octagons where the <110> facets cannot be detected. Similarly, the <111> projected shapes of cube, truncated rhombic dodecahedron, over-truncated cuboctahedron, and cantellated octahedron are all hexagons. For this reason, we only characterized nanoparticles with the <110> direction parallel to the electron beam.

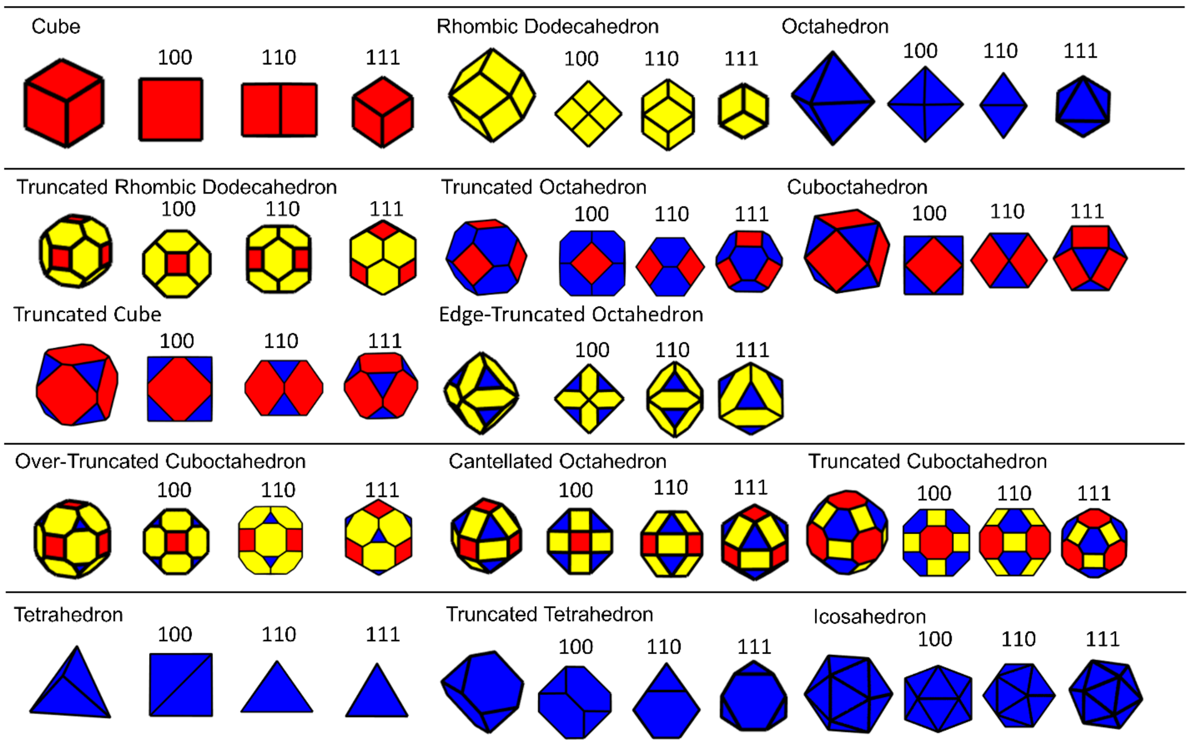

Figure S1. 3D polyhedron models used in this investigation. Red, yellow, and blue represent <100>, <110>, and <111> facets, respectively. To the right of each 3D shape are the 2D shapes as observed from the <100>, <110>, and <111> viewing directions.

The geometric relationship between the edge lengths of the <110>-projected polygonal shapes of these selected polyhedra and surface areas of <100>, <110>, and <111> facets is computed from the geometric models. The surface area of each facet can be quantitively computed for experimental particles by measuring the edge length of the traced profile of each nanoparticle. Tables S2, S3, and S4 give the analytical expressions for each polyhedron. The variables a, b, c, d, and e represent the lengths of a particular edge, with crystallographic orientation (plane normal) of that edge designated in parentheses. The angle between two adjacent edges is also annotated. Though different shapes have different equations, the equations of some shapes can be generalized to others with some geometric constraints. In Table S2, the equations for the truncated cuboctahedron can be reduced to equations for other shapes; for example, setting $c = 0$ will lead to the equations for the truncated octahedron. The <110>-projected truncated octahedron has a hexagonal shape which is different from octagonal shape projected from the truncated cuboctahedron. This difference can be detected in TEM images. However, if a constraint of $a = (\sqrt{3}/2)b$ is added, the equations for the truncated octahedron are reduced to the equations for the cuboctahedron. Due to the resolution limit of TEM, this condition $a = (\sqrt{3}/2)b$ may not be exactly measured, so that cuboctahedron can be regarded as a special case of the truncated octahedron. Similarly, Tables S3 and S4 summarize the other two groups of equations. Here, a truncated cuboctahedron is defined as the Wulff shape that has all three of the lowest-energy facets: <111>, <110>, and <100>. The over-truncated cuboctahedron means that the <110> facets account for the majority of the surface area, leaving only a smaller area fraction of <111> facets.

Table S2. Equations used to calculate the surface area of <111>, <110>, and <100> facets from projected shapes. Note that the equations for the truncated cuboctahedron (top row) can be generalized to describe other shapes (other rows) by the addition of one or more geometric constraints (shown in red for each shape).

Shape	Projection	Area	Geometric Constraints
Truncated Cuboctahedron 	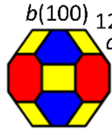	$S(100) = 6b^2 - 6c^2$ $S(111) = (8\sqrt{3}/3)a^2 + 8ab - 4\sqrt{3}b^2 - 8\sqrt{2}ac + 8\sqrt{6}bc - 8\sqrt{3}c^2$ $S(110) = 8\sqrt{3}ac - 12bc + 12\sqrt{2}c^2$	
Cantellated Octahedron 		$S(100) = 3b^2$ $S(111) = (8\sqrt{3}/3)a^2$ $S(110) = 4\sqrt{6}ab$	$c = (\sqrt{2}/2)b$
Truncated Octahedron 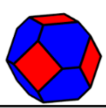	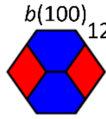	$S(100) = 6b^2$ $S(111) = (8\sqrt{3}/3)a^2 + 8ab - 4\sqrt{3}b^2$ $S(110) = 0$	$c = 0$
Cuboctahedron 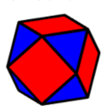	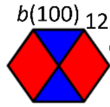	$S(100) = 6b^2$ $S(111) = (8\sqrt{3}/3)a^2$ $S(110) = 0$	$c = 0$ & $a = (\sqrt{3}/2)b$
Truncated Cube 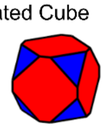	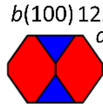	$S(100) = 6b^2 - 6c^2$ $S(111) = (8\sqrt{3}/3)a^2$ $S(110) = 0$	$a = (\sqrt{3}/2)b - (\sqrt{6}/2)c$
Cube 	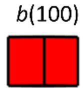	$S(100) = b^2 + 4c^2$ $S(111) = 0$ $S(110) = 0$	$a = 0$ & $b = \sqrt{2}c$
Octahedron 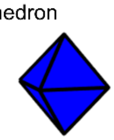	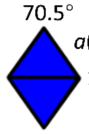	$S(100) = 0$ $S(111) = (8\sqrt{3}/3)a^2$ $S(110) = 0$	$b = c = 0$

Table S3. Equations used to calculate the surface area of <111>, <110>, and <111> facets from projected shapes. Similar to Table S2, the equations for the over-truncated cuboctahedron (top row) can be generalized to other shapes (all other rows) by the addition of one or more geometric constraints (shown in red for each shape).

Shape	Projection	Area	Geometric Constraints
Over-Truncated Cuboctahedron 	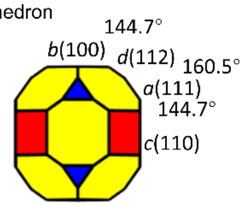	$S(100) = 3b^2$ $S(111) = (8\sqrt{3}/3)a^2$ $S(110) = (8\sqrt{3})ac + (12c + 6\sqrt{2}b)\sqrt{d^2 - (\frac{1}{2}c - \frac{\sqrt{2}}{4}b)^2}$	$d = \frac{\sqrt{3}}{2}c - \frac{\sqrt{6}}{4}b$
Truncated Rhombic Dodecahedron 	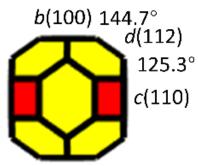	$S(100) = 3b^2$ $S(111) = 0$ $S(110) = (12c + 6\sqrt{2}b)\sqrt{d^2 - (\frac{1}{2}c - \frac{\sqrt{2}}{4}b)^2}$	$a = 0$
Edge-Truncated Octahedron 	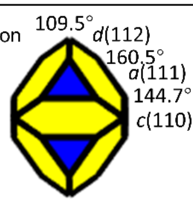	$S(100) = 0$ $S(111) = (8\sqrt{3}/3)a^2$ $S(110) = (8\sqrt{3})ac + 12c\sqrt{d^2 - \frac{1}{4}c^2}$	$b = 0$
Rhombic Dodecahedron 	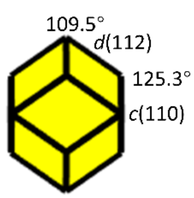	$S(100) = 0$ $S(111) = 0$ $S(110) = 12c\sqrt{d^2 - \frac{1}{4}c^2}$	$a = b = 0$

Table S4. Equations used to calculate the surface area of <111>, <110>, and <111> facets from projected shapes. The equations for the truncated tetrahedron can be generalized to describe other shapes through the addition of geometric constraints (shown in red). The icosahedron is not a Wulff polyhedron, but its area can be computed using simple geometry.

Shape	Projection	Area	Geometric Constraints
Truncated Tetrahedron 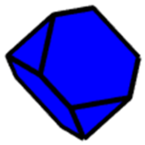	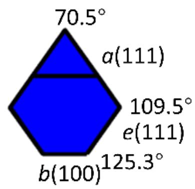	$S(100) = 0$ $S(111) = 2ab + (8\sqrt{3}/3)ae + 2be$ $S(110) = 0$	
Tetrahedron 	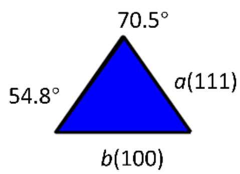	$S(100) = 0$ $S(111) = (2\sqrt{3}/3)a^2 + (\sqrt{3}/2)b^2$ $S(110) = 0$	$e = 0$ & $b = (2\sqrt{3}/3)a$
Icosahedron 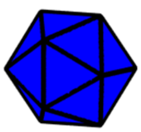	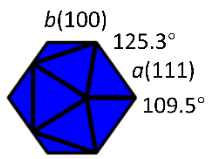	$S(100) = 0$ $S(111) = 10\sqrt{3}b^2$ $S(110) = 0$	$a = \sqrt{2}b$

S3. Simulation Details

The relationship between size and number of atoms for the truncated octahedron and truncated cuboctahedron nanoparticle is plotted in Fig. S2a. The relative surface area fraction of these shapes is plotted in Fig. S2b.

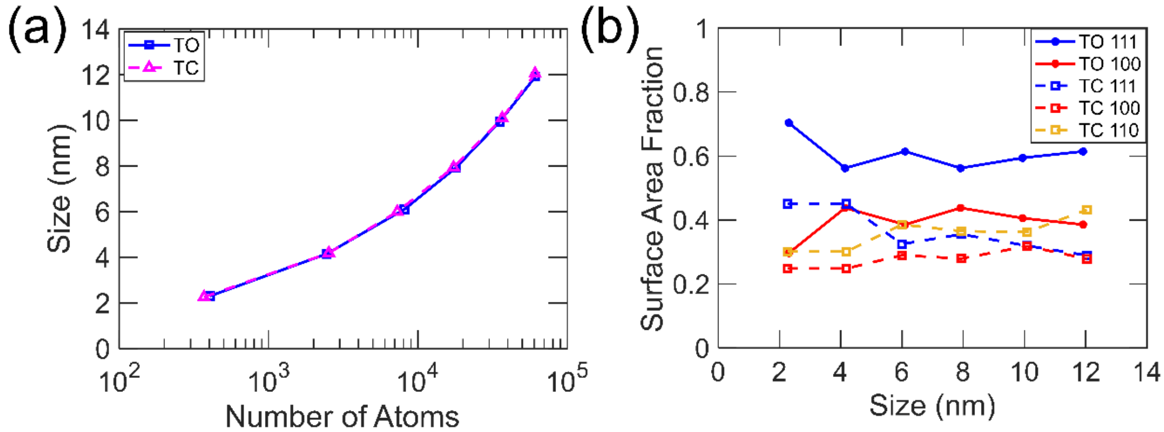

Figure S2. Details of the model truncated octahedron (TO) and truncated cuboctahedron (TC) particles of varying sizes (a) and the surface area fraction of these shapes (b). The particle size is defined as the equivalent diameter of the shapes as observed along the <110> viewing direction.

The MD simulations were also equilibrated at the two other temperatures involved in synthesis, 250℃ and 675℃ to look for structural changes. Specifically, after creation of the particles (TO and TC at all sizes), the energy minimization and equilibration process was repeated, as described in the main text, at temperatures of 250°C and 675°C. As shown in Fig. S3, atomic vibration at the surface was observed, but there were no structural changes in the shape of the nanoparticle. The edges, corners, and overall geometric features of the nanoparticles were preserved over time even at the highest temperature of our models.

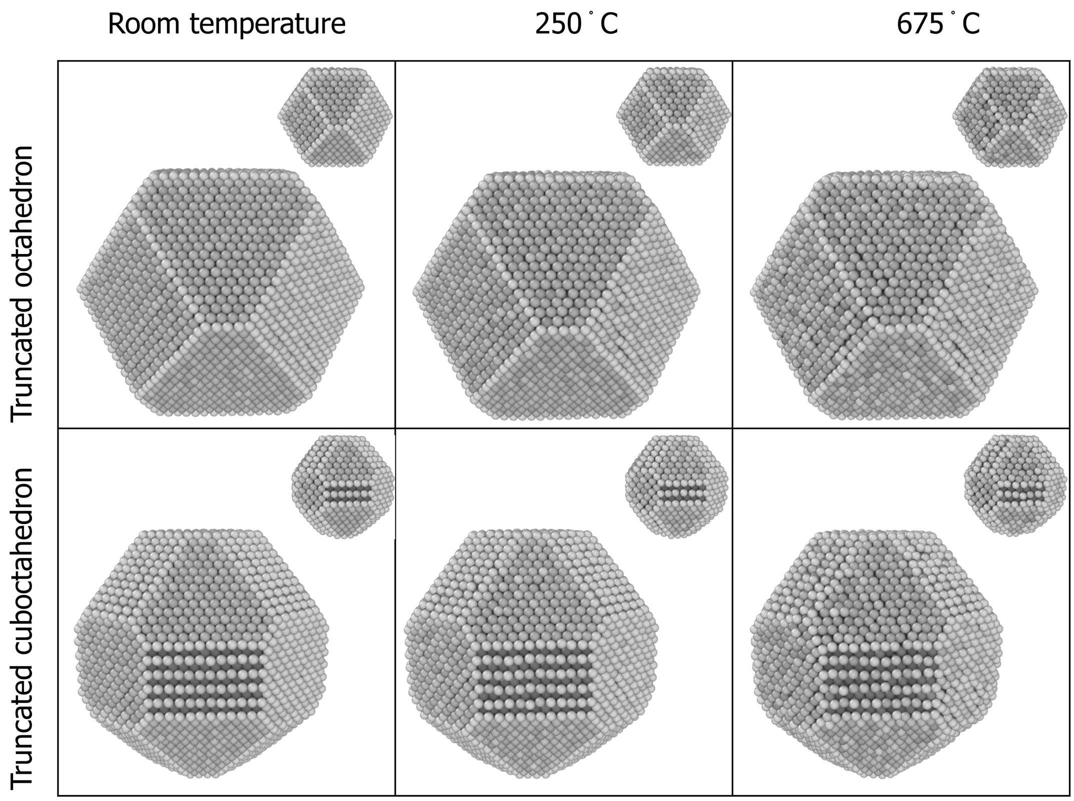

Figure S3. To check for structural changes at elevated temperature, all particles were equilibrated at the three different temperatures that were involved in synthesis. While all of the particles at all sizes were subjected to this analysis, only the largest and smallest particles are shown here as representatives. Both particles are shown for the truncated octahedron (top row) and truncated cuboctahedron (bottom row) at all three temperatures (represented by the columns). While increased atomic motion is clearly visible, with increased waviness introduced into rows of atoms in a given plane, there is no bulk structural changes to the particles. In all cases, the particle shape is maintained. The thermal fluctuation of the nanoparticles during MD simulation is shown in Fig. S4. After the first few picoseconds, the deviation is small, which confirms thermal equilibrium was reached within the simulation time.

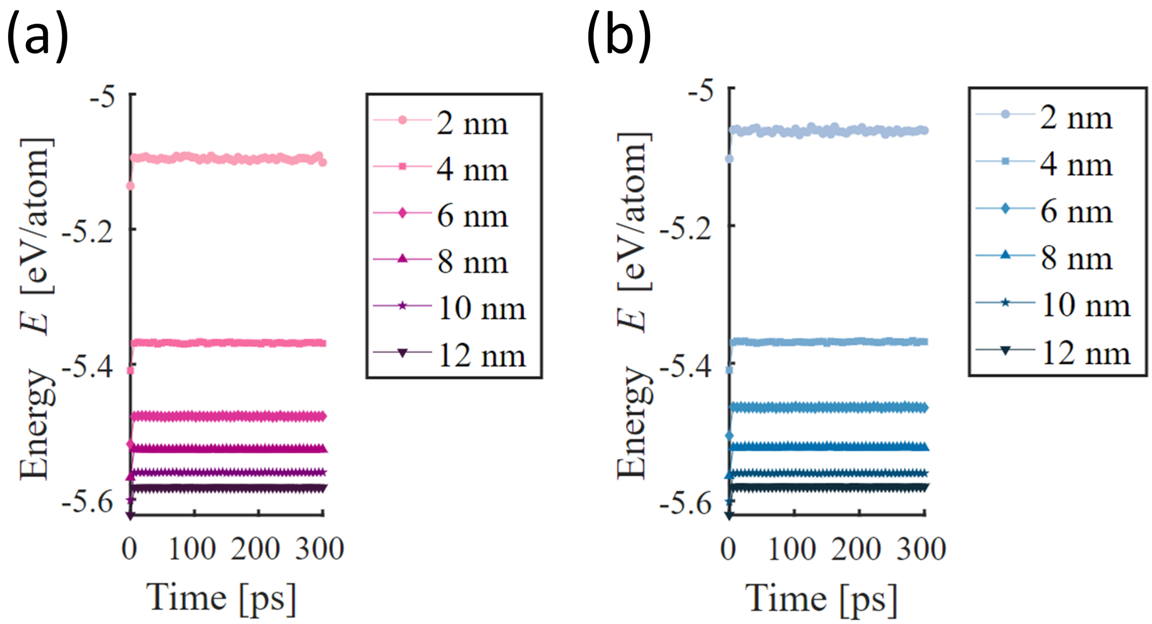

Figure S4. The energy change with time during MD simulations in Fig. 4(b) of truncated octahedron (a) and truncated cuboctahedron (b) nanoparticles of varying sizes.

References

1 Y. H. Wen, H. Fang, Z. Zhu and S. G. Sun, *Phys. Lett. Sect. A Gen. At. Solid State Phys.*, 2009, **373**, 272–276.

2 R. Huang, Y. H. Wen, Z. Z. Zhu and S. G. Sun, *J. Mater. Chem.*, 2011, **21**, 11578–11584.

3 J. H. Shim, B. J. Lee and Y. W. Cho, *Surf. Sci.*, 2002, **512**, 262–268.

4 F. Baletto, R. Ferrando, A. Fortunelli, F. Montalenti and C. Mottet, *J. Chem. Phys.*, 2002, **116**, 3856–3863.

5 A. S. Barnard, X. M. Lin and L. A. Curtiss, *J. Phys. Chem. B*, 2005, **109**, 24465–24472.

6 B. Fleury, R. Cortes-Huerto, O. Taché, F. Testard, N. Menguy and O. Spalla, *Nano Lett.*, 2015, **15**, 6088–6094.

7 J. M. Rahm and P. Erhart, *Nano Lett.*, 2017, **17**, 5775–5781.

8 K. Koga and K. Sugawara, *Surf. Sci.*, 2003, **529**, 23–35.

9 A. S. Barnard and L. A. Curtiss, *ChemPhysChem*, 2006, **7**, 1544–1553.

10 G. Wulff, *Zeitschrift für Krist.*, 1901, **34**, 449–530.

11 W. Gao, J. Wu, A. Yoon, P. Lu, L. Qi, J. Wen, D. J. Miller, J. C. Mabon, W. L. Wilson, H. Yang and J. M. Zuo, *Sci. Rep.*, 2017, **7**, 1–10.